Scattering Studies of Nanoporous Organosilicate Thin Films Imprinted with Reactive Star Porogens

B. Lee,[†,⊥] W. Oh,[†,⊥] J. Yoon,[†,⊥] Y. Hwang,[†] J. Kim,[†] B. G. Landes,[‡] J. P. Quintana,[§] and M. Ree*[,†]

National Research Lab for Polymer Synthesis & Physics, Pohang Accelerator Laboratory, Center for Integrated Molecular Systems, Department of Chemistry, Polymer Research Institute, and Division of Molecular and Life Sciences, and School of Environmental Science & Engineering, Pohang University of Science & Technology, Pohang 790-784, Republic of Korea; Department of Analytical Sciences-Materials Characterization, 1897 Building, Dow Chemical Company, Midland, Michigan 48667; and DND-CAT Synchrotron Research Center, Building 432A/A-008, Argonne National Laboratory, 9700 S. Case Ave., Argonne, Illinois 60439-4857

Received January 30, 2005

Revised Manuscript Received September 15, 2005

Low dielectric constant (low-k) dielectric materials not only lower line-to-line noise in interconnect conductor lines but also minimize power dissipation by reducing the capacitance between the interconnect conductor lines.[1] Thus, low-k dielectrics ($k < 2.5$) are highly sought after by the microelectronics industry, which is rapidly developing advanced integrated circuits (ICs) that have improved functionality and speed in smaller packages and that consume less power.[1] Because most organic and inorganic materials have dielectric constants of $k > 2.8$, considerable effort has been devoted to reducing the k value of dielectric materials by incorporating air, the medium with the lowest possible dielectric constant ($k = 1.01$), into these materials as pores.[1−4] One promising approach is imprinting pores in organosilicates such as poly(methylsilsesquioxane) (PMSSQ) ($k = 2.7$) by sacrificial degradation of organic porogens at 350−450 °C.[2−5] However, the tendency of porogens to aggregate in organosilicates has limited the pore size reduction and porosity of the resulting dielectrics,[2−5] making them unsuitable for use in advanced ICs with small feature sizes. In particular, star-shaped porogens with a high number of arms show a severe aggregation, even at porogen loadings as low as 10−20 wt %, generating large and interconnected pores in the dielectric thin films.[4,5] Thus, if such advanced ICs are to be developed, a method is needed for generating dielectric materials containing a uniform distribution of closed pores with a pore size much smaller than the feature size of the ICs. Moreover, the ability to characterize the pore structure in porous dielectrics is as important as developing the dielectrics and porogens themselves.

In this study, we aimed to minimize aggregation of a star-shaped poly(ϵ-caprolactone) porogen with four arms in a PMSSQ dielectric matrix by chemical modification of the porogen end groups. To test the efficacy of the proposed modification, the nanostructures and properties of porous dielectrics prepared using different amounts of the modified porogen were quantitatively characterized.

A soluble PMSSQ precursor containing reactive ethoxysilyl and hydroxysilyl groups was used as the dielectric material, while a four-armed poly(ϵ-caprolactone) with and without triethoxysilyl termination (mPCL4 and PCL4) were used as thermally labile porogens (Figure 1). PCL4 (6800 $\overline{M}_w$ (weight-average molecular weight) with a polydispersity index (PDI) of 1.10 and an average degree of polymerization per arm of 8.9) was synthesized by the di(trimethylol propane)-initiated polymerization of ϵ-caprolactone, catalyzed by stannous 2-ethylhexanoate, according to a previously reported method.[4−6] The hydroxyl end groups of PCL4 were further chemically modified by reaction with 3-isocyanatopropyltriethoxysilane, producing triethoxysilyl-terminated porogen (mPCL4).[7] On heating, thermogravimetric analysis found that the mPCL4 porogen's triethoxysilyl terminal groups undergo curing reaction over the temperature region 110−285 °C, with loss of sample weight due to the evaporation of ethanol byproduct, and the porogen decomposes over the temperature region 290−375 °C. The PMSSQ precursor (10 000 $\overline{M}_w$, supplied by Techneglas Co.)[8] used in our study was found to undergo curing reaction over the temperature region 75−340 °C, which is accompanied by weight losses due to the evaporation of the water and ethanol byproducts, and the cured PMSSQ dielectric is stable up to 500 °C. Because of the overlapping of the temperature regions in which the curing reactions of the PMSSQ precursor and the mPCL4 porogen occur, favorable chemical hybridization is likely to occur in their blends, which minimizes the aggregation of porogen molecules that can occur prior to their sacrificial thermal decomposition. In comparison, the unmodified PCL4 porogen was found to decompose over 205−352 °C.

Taking these results into account, we prepared porous PMSSQ dielectric films on precleaned Si(100) wafers from the PMSSQ precursor and the porogens (Figure 1).[9] PMSSQ/porogen blend films were additionally prepared by partial curing at 200 °C for 100 min in a vacuum. The thicknesses of films were ca. 700 nm. 2D GISAXS measurements were performed in a vacuum using an X-ray beam (0.8×0.6 mm^2) of 7.25 keV at the 4C1 SAXS Beamline[10] of the Pohang Accelerator Laboratory, and 2D TSAXS experiments were conducted in a vacuum using an X-ray beam (0.5×0.3 mm^2) of 15.00 keV at the DND-CAT Synchrotron Research Center[11] of the Argonne National Laboratory. 2D charge-coupled device detectors were used, and the sample-to-detector distance was 1.00 and 2.50 m for GISAXS and 4.30 m for TSAXS. In addition, PMSSQ dielectric films of ca. 700 nm thick were prepared by curing at 400 °C and by partial curing at 200 °C in a vacuum, and their TSAXS and GISAXS patterns were measured and used as a background run data for correcting the scattering data of the porous PMSSQ films and the partially cured blend films. The dielectric films were further characterized by using a Woollam ellipsometer and an Agilent impedance analyzer. Transmission electron microscopy (TEM) measurements were carried out using a JEM microscope on samples prepared on carbon grids.

Figure 2 shows a representative TEM image of a porous PMSSQ film. The TEM image clearly shows that

† Pohang University of Science & Technology.
‡ Dow Chemical Company.
§ Argonne National Laboratory.
⊥ These authors contributed equally to this work.
* To whom all correspondence should be addressed: Tel +82-54-279-2120; Fax +82-54-279-3399; e-mail ree@postech.edu.

10.1021/ma0501951 CCC: $30.25
Published on Web 09/30/2005

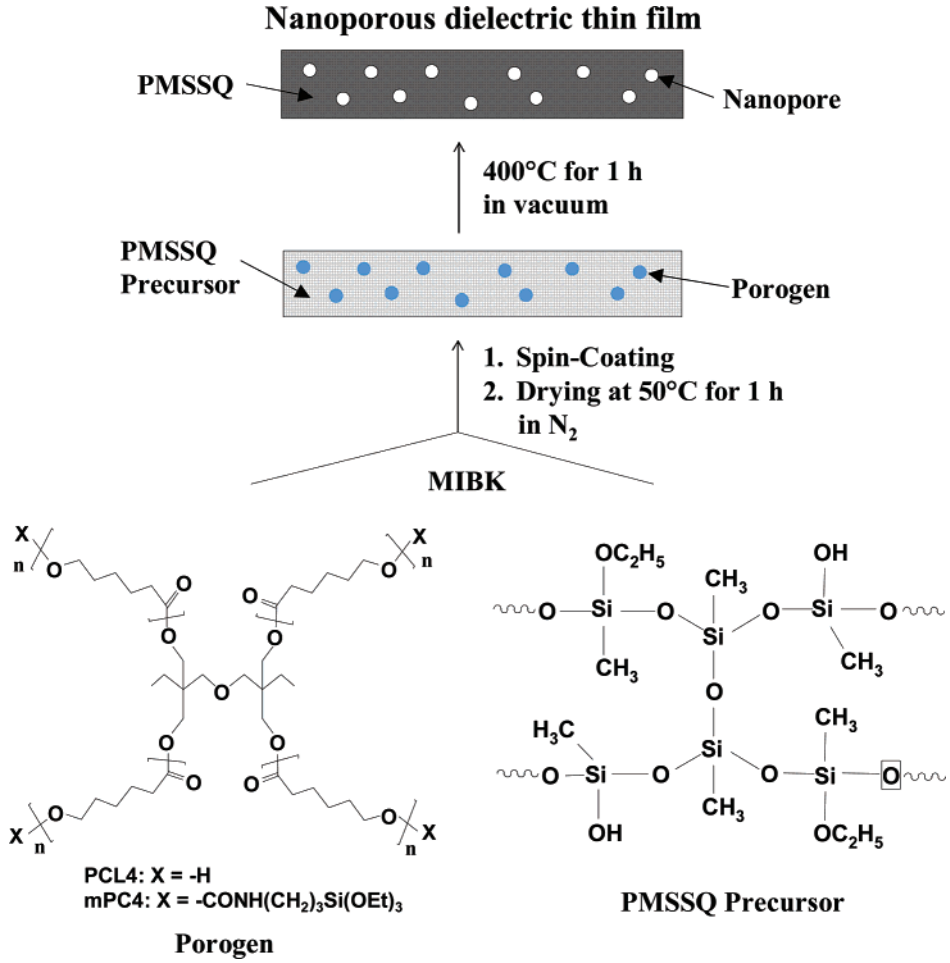

Figure 1. Procedure for preparing nanoporous organosilicate thin films from a curable PMSSQ precursor (10 000 $\overline{M_w}$: weight-average molecular weight) and a thermally labile star-shaped molecule, mPCL4 [$\overline{M_w}$ = 8000, PDI (polydispersity index) = 1.11, and DP (degree of polymerization)/arm = 8.9], or PCL4 ($\overline{M_w}$ = 6800, PDI = 1.10, and DP/arm = 8.9).

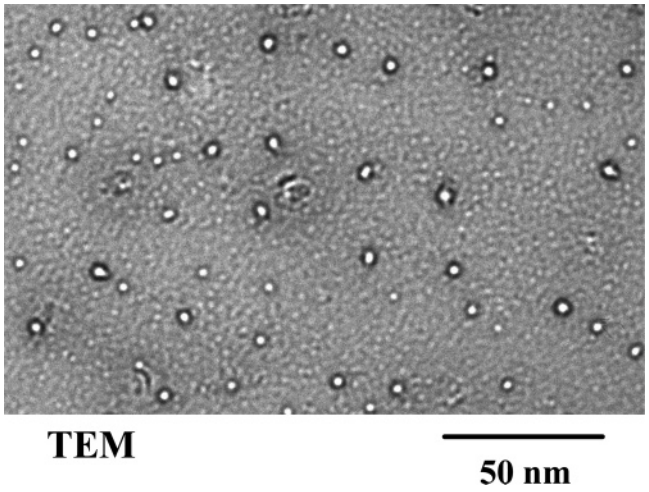

Figure 2. TEM image of a nanoporous PMSSQ dielectric imprinted with 10.0 wt % mPCL4 porogen.

the nanopores generated in the dielectric film by the sacrificial thermal degradation of the mPCL4 porogen are spherical in shape and that their sizes are around 6 nm. Similar TEM images were obtained for porous PMSSQ films imprinted with the PCL4 porogen, but the pore sizes are larger in comparison to those prepared with the mPCL4 porogen (data not shown).

Figure 3a shows a representative 2D TSAXS pattern, which was measured for a 700 nm thick PMSSQ film imprinted with 30 wt % mPCL4, and for comparison, Figure 3b shows the 2D GISAXS pattern measured with an X-ray beam incident at a grazing angle α_i (=0.20°) for the same sample. The 2D TSAXS pattern appears isotropic, indicating that the pores are randomly distributed in the in-plane of the porous film. The 2D GISAXS pattern reveals bright scattering features along the $2\theta_f$ axis direction at an α_f region between the critical angles of the film and silicon substrate ($\alpha_{c,f}$ and $\alpha_{c,s}$), which are intense scattering due to a type of standing wave phenomenon and total reflection at the interface between the film and the substrate. Except for such bright scattering features between the $\alpha_{c,f}$ and $\alpha_{c,s}$, the 2D GISAXS pattern shows no preferential orientations, confirming that the pores are randomly distributed in the in-plane and out-of-plane of the porous film. Similar TSAXS and GISAXS patterns were obtained for the films imprinted with other loadings of mPCL4 and those prepared with PCL4. Considering these results, we extracted in-plane GISAXS profiles along the $2\theta_f$ axis direction at an exit angle α_f (0.20°) between the $\alpha_{c,f}$ and $\alpha_{c,s}$ values from the measured 2D GISAXS patterns, which can give structural information in the film plane, and compared them with the 1D TSAXS profiles obtained from the measured 2D TSAXS patterns, which can also provide structural information in the film plane (Figure 4).

The extracted in-plane GISAXS profiles can be analyzed using the GISAXS formula[5] derived for particles

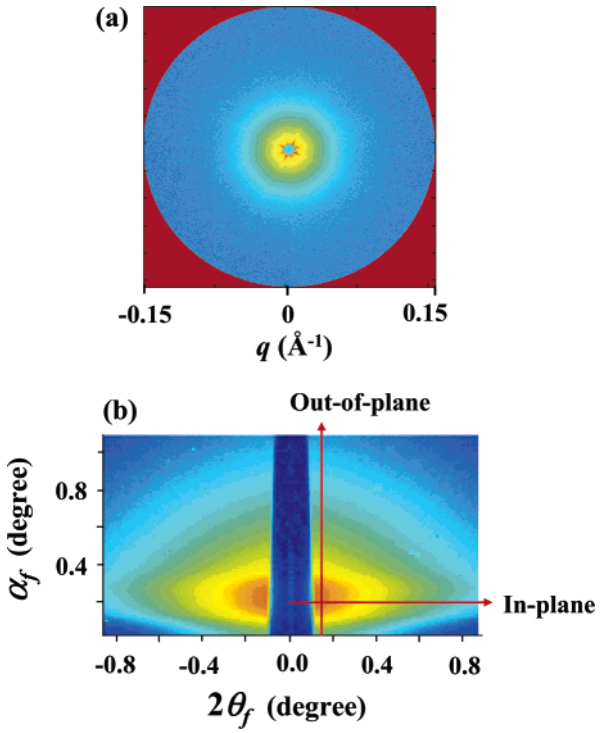

Figure 3. Representative scattering patterns measured for a 700 nm thick porous PMSSQ film imprinted with 30 wt % mPCL4 porogen: (a) TSXAS pattern; (b) GISAXS pattern. Double-side polished, 70 μm thick Si wafers (25 mm diameter) were used a substrate. α_f is the angle between the scattered beam and the film surface (i.e., the out-of-plane exit angle), and $2\theta_f$ is the angle between the scattered beam and the plane of incidence (i.e., the in-plane exit angle).

buried in a film on a substrate. To analyze the extracted in-plane GISAXS profiles by using the GISAXS formula, we considered all possible scattering models for the scattered intensity from pores in the dielectric film (i.e., I_1 term in the GISAXS formula[5]) and then found that the hard-sphere model[12] with a log−normal size distribution is the most suitable for analyzing the measured GISAXS profiles. As seen in Figure 4, the in-plane GISAXS profiles of the porous films imprinted with the mPCL4 porogen are well fitted with the GISAXS formula of the hard-sphere model. In contrast, although the scattering profiles of the films imprinted with 10−20 wt % PCL4 loadings can be reasonably well fitted with the GISAXS formula of the hard-sphere model, those of the films prepared with higher PCL4 loadings (>20 wt %) could not be fitted with the GISAXS formula. On the other hand, we found that the 1D TSAXS profiles are well fitted with the hard-sphere model with the log−normal pore size distribution, rather than any other scattering models (Figure 4). These GISAXS and TSAXS results collectively indicate that the pores in the porous films are spherical and have a sharp interface with the PMSSQ matrix.

From our analyses of the GISAXS and TSAXS profiles, we determined the size and size distribution of pores in the porous films (Table 1 and Figure 5). Overall, the pore size and size distribution determined from the GISAXS data were in reasonably good agreement with those obtained from the TSAXS data. For films imprinted with PCL4, the average radius of gyration $\overline{R_g}$ of the pores increased substantially, from 4.4 to 5.3 to >40 nm, as the porogen loading was increased from 10 to 30 wt %. These results indicate that, consistent with

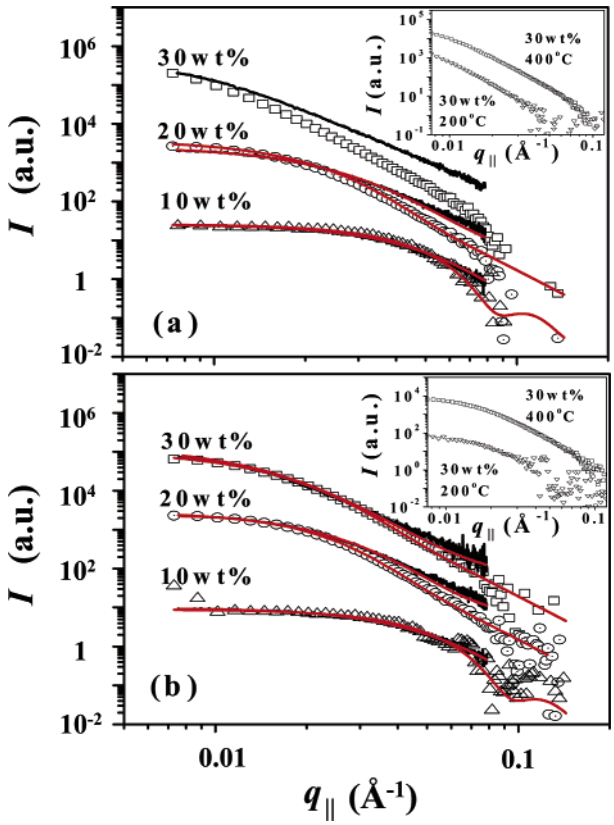

Figure 4. 1D SAXS profiles obtained from 2D SAXS patterns of porous PMSSQ films. (a) 1D SAXS profiles of porous films imprinted with PCL4; inset: TSAXS profiles measured before and after the sacrificial thermal degradation of PCL4 loaded in a film. (b) 1D SAXS profiles of porous films imprinted with mPCL4; inset: TSAXS profiles measured before and after the sacrificial thermal degradation of mPCL4 loaded in a film. The percentages indicate the initial porogen loadings. Symbols are the TSAXS profiles while solid lines (black color) are the in-plane GISAXS profiles; the solid lines (red color) were obtained by fitting the data with the scattering formulas. The GISAXS profiles were extracted along the $q_{||}$ direction at $\alpha_f = 0.20°$ from the 2D GISAXS patterns.

previous reports,[3−5] PCL4 tends to undergo severe aggregation in the PMSSQ matrix at loadings greater than 20 wt %, creating large pores in the film. Compared to PCL4, mPCL4 was found to give pores of smaller size and narrower size distribution, with $\overline{R_g}$ values in the range 4.0−17.1 nm for mPCL4 loadings of up to 30 wt %. These results indicate that severe aggregation of mPCL4 is suppressed in the PMSSQ matrix. This suppression of mPCL4 aggregation can be attributed to the triethoxysilyl terminal groups of the porogen, which are analogues of the reactive functional groups of the PMSSQ precursor that take part in the curing reaction during the film formation process (Figure 1). Because of the similarity of the two types of groups, mPCL4 is more miscible with the PMSSQ precursor than is PCL4, and furthermore, the triethoxysilyl terminal groups cause the porogen to participate in the curing reaction of the PMSSQ precursor, leading to a significant inhibition of aggregation in the mPCL4/PMSSQ system.

In addition, the TSAXS scattering profiles of a given sample were almost the same before and after sacrificial thermal degradation of the porogen, except for some differences in intensity (insets in Figure 4). This similarity in the profiles indicates that the distribution of porogen molecules in the PMSSQ matrix after drying and partial curing is retained without further aggrega-

Table 1. Pore Structures and Properties of Nanoporous PMSSQ Films Imprinted with mPCL4 and PCL4 Porogens

porogen loading (wt %)	cure temp (°C)	$\overline{R_g}$[a] (nm) TSAXS	$\overline{R_g}$[a] (nm) GISAXS	ρ_e[b] (nm^{-3})	P[c] (%)	n[d]	k[e]
0	400			399		1.3960	2.70
mPCL4							
10	400	4.0 (0.04)[f]	5.2 (0.01)[f]	376	5.8	1.3620	2.45
20	400	10.1 (0.05)	10.0 (0.02)	340	14.8	1.3214	2.16
30	400	14.8 (0.09)	17.1 (0.03)	297	25.6	1.2921	1.95
30	200	14.8 (0.09)		396			
PCL4							
10	400	4.4 (0.06)	5.3 (0.01)	373	6.5	1.3587	2.44
20	400	11.3 (0.10)	10.0 (0.02)	338	15.3	1.3207	2.16
30	400	>40[g]	>40[g]	302	24.3	1.2795	1.85
30	200	>40[g]		398			

[a] Average radius of gyration estimated from the radius r and number distribution of pores obtained by the analysis of SAXS profile. [b] Electron density determined from the out-of-plane GISAXS profile. [c] Porosity estimated from the electron density of the film. [d] Refractive index measured at 633 nm using spectroscopic ellipsometry. [e] Dielectric constant measured at 1 MHz using an impedance analyzer. [f] Standard deviation in the determined $\overline{R_g}$ value. [g] Not detected due to the out of the detection limit (ca. 40 nm).

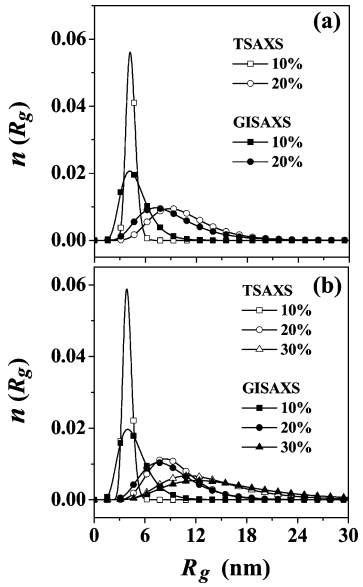

Figure 5. Pore radius and distribution determined from the scattering profiles in Figure 4: (a) porous films imprinted with PCL4; (b) porous films imprinted with mPCL4.

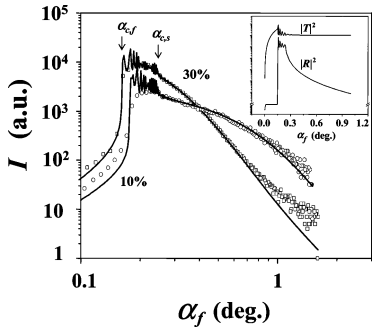

Figure 6. Out-of-plane GISAXS profiles obtained at $2\theta_f = 0.156°$ from 2D GISAXS patterns of porous PMSSQ films imprinted with mPCL4; the percentages indicate the initial porogen loadings, the symbols are the measured data, and the solid lines were obtained by fitting the data with the GISAXS formula.

tion through the curing/calcination process, and hence the pores imprinted in the cured film are of the same dimensions as those of the dispersed or partially aggregated porogen molecules that form during the drying and partial curing process.

Here it is further noted that, as seen in Figure 4, the in-plane GISAXS and TSAXS profiles are similar for the films imprinted with 10 wt % loadings of PCL4 or mPCL4 but show deviations for the films prepared with higher porogen loadings. These deviations are mainly due to the following two factors. First, the cross-section area of a film irradiated by an X-ray beam incident at a grazing angle (for example, $\alpha_i = 0.20°$), as in GISAXS measurements, is much larger than that in TSAXS measurements. The sampling volume of TSAXS corresponds to the X-ray beam size (0.5×0.3 mm^2) times the film thickness (700 nm), whereas that of GISAXS is the product of the X-ray beam width (0.8 mm), the film thickness (700 nm), and the X-ray beam path length in the film (i.e., X-ray beam footprint length) (25 mm) because in our GISAXS measurement the footprint of the X-ray beam is larger than the length of the film sample. Second, the in-plane GISAXS profiles consist of three scattering components—one $q_{||}$ component (i.e., q_y) and two q_z components, $q_{1,z}$ and $q_{2,z}$, which correspond to the q_z components of scattering vectors by the transmitted and reflected beam, respectively[5]—whereas the 1D TSAXS profiles consist of a single scattering component (i.e., q_y). In the case of $\alpha_i = 0.20°$ and $\alpha_f = 0.18°$, $q_{1,z}$ can be calculated to be very small (0.01 $Å^{-1}$) when refraction of the incident beam in the film is taken into account; $q_{2,z}$ is zero. In contrast to $q_{1,z}$, $q_{||}$ is not changed by refraction of the incident beam in the film. Furthermore, the pores in the porous dielectric films of our study are small but have relatively broad size distributions. For a given dielectric film, the in-plane scattering profiles at various α_f values between $\alpha_{c,f}$ and $\alpha_{c,s}$ were found to be identical except for some differences in intensity. The factors and findings outlined above indicate that the contributions of the q_z components to the overall **q** are negligible compared to that of the $q_{||}$ component. We therefore conclude that the deviations in the in-plane GISAXS and TSAXS profiles are caused by differences in the X-ray irradiated areas of the porous films in the GISAXS and TSAXS measurements. Consequently, such deviations indicate a macroscopic inhomogeneity in the pore distribution in the films. Given that greater deviations were observed for the films imprinted with PCL4, compared to those prepared with mPCL4 (Figure 4), we conclude that the distribution of pores is much more inhomogeneous in the porous films imprinted with PCL4 than in those imprinted with mPCL4.

Figure 6 shows the out-of-plane GISAXS profiles for PMSSQ films imprinted with 10 and 30 wt % mPCL4. Similar GISAXS profiles were obtained for the other porous films (data not shown). The scattering profiles

were well fitted by the GISAXS formula along with the pore parameters obtained from the analysis of the in-plane GISAXS profiles, confirming that the pore size and pore size distribution are isotropic in the dielectric films. These results indicate that the procedure used—spin-coating, drying, and thermal processing—does not induce any anisotropy in the pore shape and size in the nanoporous films.

The scattering profiles (Figure 6) further show intense scattering features in the α_f region of 0.15°−0.28°, which are due to the standing wave phenomenon and total reflection at the interface between the film and the substrate as discussed above. In general, such intense scattering features appear in an oscillation mode whose frequency period relates to the film thickness. However, the thicknesses of the films used in the measurements are 700 nm, which is too thick and thus causes a high frequency of oscillations in the scattering. Because of the high frequency, oscillations apparently are not easily discernible in the scattering profiles. Such intense scattering features of a high-frequency oscillation result from the $|R|^2$and $|T|^2$ terms in the GISAXS formula (see the calculated $|R|^2$ and $|T|^2$ profiles in the inset of Figure 6); here, R and T are the reflected and transmitted amplitudes of the X-ray beam (i.e., incoming or outgoing X-ray beam), respectively. These terms' profiles provide the α_cs of the film and silicon substrate. The $\alpha_{c,f}$ of the film clearly decreases with increasing initial porogen loading (Figure 6). From the $\alpha_{c,f}$ values, the film electron density of each film was determined and then used to estimate the film porosity. The porosities of the films ranged from 5.8% to 25.6% (Table 1). As the porosity of the PMSSQ film increases, the values of k and n (refractive index) decrease (Table 1).

In summary, the results of this study highlight the potential of reactive triethoxysilyl modification of the end groups of four-armed porogen as a means of preventing severe aggregation of star-shaped porogen with multiple arms in the preparation of ultralow-k nanoporous poly(alkylsilsesquioxane) dielectric films from the soluble poly(alkylsilsesquioxane) precursors having ethoxylsilyl and hydroxy groups which can underogo curing reaction. In addition, we first reported that GISAXS combined with conventional TSAXS can quantitatively characterize the structures and properties of ultralow-k nanoporous dielectric thin films on substrates, providing the pore shape, size, size distribution, and the inhomogeneity and anisotropy of the pore distribution as well the electron density and porosity. In particular, it was demonstrated that GSAXS is a very powerful tool to characterize the nanostructure and properties of nanoscale thin films.

Acknowledgment. This study was supported by the Korea Science & Engineering Foundation (NRL Program: Contract 2005-01385) and by the Korean Ministry of Education (BK21 Program). GISAXS measurements at Pohang Accelerator Laboratory were supported by MOST and POSCO. TSAXS measurements at the DND-CAT of Argonne National Laboratory were supported by the E. I. DuPont de Nemours & Co., the Dow Chemical Co., the U.S. National Science Foundation (Grant DMR-9304725), the State of Illinois (Department of Commerce), the Board of Higher Education (Grant IBHE HECA NWU 96), and the U.S. Department of Energy (Basic Energy Sciences and Office of Energy Research under Contract W-31-102-Eng-38).

References and Notes

(1) (a) *International Technology Roadmap for Semiconductors*; Semiconductor Industry Association: San Jose, CA, 2001. (b) Miller, R. D. *Science* **1999**, *286*, 421. (c) Maex, K.; Baklanov, M. R.; Shamiryan, D.; Iacopi, F.; Brongersma, S. H.; Yanovitskaya, Z. S. *J. Appl. Phys.* **2003**, *93*, 8793. (d) Morgen, M.; Ryan, E. T.; Zhao, J.-H.; Hu, C.; Cho, T.; Ho, P. S. *Annu. Rev. Mater. Sci.* **2000**, *30*, 645. (e) Maier, G. *Prog. Polym. Sci.* **2001**, *26*, 3.

(2) (a) Huang, E.; Toney, M. F.; Volksen, W.; Mecerreyes, D.; Brock, P.; Kim, H.-C.; Hawker, C. J.; Hedrick, J. L.; Lee, V. Y.; Magbitang, T.; Miller, R. D. *Appl. Phys. Lett.* **2002**, *81*, 2232. (b) Lee, H.-J.; Lin, E. K.; Wang, H.; Wu, W.-L.; Chen, W.; Moyer, E. C. *Chem. Mater.* **2002**, *14*, 1845. (c) Yang, S.; Mirau, P. A.; Pai, C.-S.; Nalamasu, O.; Reichmanis, E.; Lin, E. K.; Lee, H.-J.; Gidley, D. W.; Sun, J. *Chem. Mater.* **2001**, *13*, 2762. (d) Kim, H.-C.; Volksen, W.; Miller, R. D.; Huang, E.; Yang, G.; Briber, R. M.; Shin, K.; Satija, S. K. *Chem. Mater.* **2003**, *15*, 609. (e) Nguyen, C.; Hawker, C. J.; Miller, R. D.; Huang, E.; Hedrick, J. L. *Macromolecules* **2000**, *33*, 4281.

(3) (a) Bolze, J.; Ree, M.; Youn, H. S.; Chu, S.-H.; Char, K. *Langmuir* **2001**, *17*, 6683. (b) Oh, W.; Hwang, Y.-T.; Park, Y. H.; Ree, M.; Chu, S.-H.; Char, K.; Lee, J.-K.; Kim, S. Y. *Polymer* **2003**, *44*, 2519. (c) Lee, B.; Park, Y.-H.; Hwang, Y.-T.; Oh, W.; Yoon, J.; Ree, M. *Nat. Mater.* **2005**, *4*, 147. (d) Kim, J.-S.; Kim, H.-C.; Lee, B.; Ree, M. *Polymer* **2005**, *46*, 7394.

(4) (a) Nguyen, C. V.; Carter, K. R.; Hawker, C. J.; Hedrick, J. L.; Jaffe, R. L.; Miller, R. D.; Remenar, J. F.; Rhee, H.-W.; Rice, P. M.; Toney, M. F.; Trollsas, M.; Yoon, D. Y. *Chem. Mater.* **1999**, *11*, 3080. (b) Hedrick, J. L.; Miller, R. D.; Hawker, C. J.; Carter, K. R.; Volksen, W.; Yoon, D. Y.; Trollsas, M. *Adv. Mater.* **1998**, *10*, 1049.

(5) (a) Lee, B.; Yoon, J.; Oh, W.; Hwang, Y.; Heo, K.; Jin, K. S.; Kim, J.; Kim, K.-W.; Ree, M. *Macromolecules* **2005**, *39*, 3395. (b) Lee, B.; Park, I.; Yoon, J.; Park, S.; Kim, J.; Kim, K.-W.; Chang, T.; Ree, M. *Macromolecules* **2005**, *39*, 4311.

(6) Shin, Y. C.; Choi, K.-Y.; Jin, M. Y.; Hong, S.-K.; Cho, D.; Chang, T.; Ree, M. *Korea Polym. J.* **2001**, *9*, 100.

(7) PCL4 (1.20 g) was dissolved in purified tetrahydrofuran (20 mL) under a nitrogen atmosphere, and then 0.67 g (2.71 mmol) of 3-isocyanatopropyltriethoxysilane was slowly added to the solution with stirring. The reaction was carried out with stirring at 60 °C for 2 days. The reaction solution was poured into dry *n*-pentane, and then the product precipitate (i.e., mPCL4) was filtered and washed several times with *n*-pentane, followed by drying for 1 day at room temperature in a vacuum. The resulting mPCL4 product was identified using proton and carbon nuclear magnetic (^{1}H and ^{13}C NMR) and infrared spectroscopy. ^{1}H NMR (δ, $CDCl_3$): 0.63 (t, 2H), 0.81 (t, 3H), 1.20 (t, 3H), 1.37 (m, 2H), 1.61 (m, 2H), 2.28 (t, 2H), 3.15 (m, 2H), 3.25 (s, 2H), 3.62 (t, 2H), 3.79 (q, 2H), 3.95 (s, 2H), 4.03 (t, 2H), 4.85 (s, 1H). ^{13}C NMR ($CDCl_3$) δ: 7.41, 7.51, 18.25, 23.27, 24.54, 25.27, 25.50, 28.32, 32.20, 34.09, 41.54, 43.33, 58.41, 62.59, 64.11, 70.95, 156.68, 173.53. IR (cm^{-1}): 3410−3590, 2942, 2867, 1733, 1357−1465, 1162−1239. The mPCL4 product was determined to have a $\overline{M_w}$ of 8000 and a PDI of 1.11 by gel permeation chromatography.

(8) (a) Oh, W.; Shin, T. J.; Ree, M.; Jin, M. Y.; Char, K. *Macromol. Chem. Phys.* **2002**, *203*, 791. (b) Oh, W.; Ree, M. *Langmuir* **2004**, *20*, 6932.

(9) A series of homogeneous solutions of each porogen with the PMSSQ precursor in methyl isobutyl ketone (MIBK) (5 wt % solid) were prepared using porogen compositions of 10, 20, and 30 wt %. Each solution was filtered using a PTFE-membrane microfilter of pore size 0.20 μm, spin-coated onto precleaned Si(100) wafers, and then dried at 50 °C for 1 h under a nitrogen atmosphere. The dried samples were heat-treated at 400 °C for 1 h under vacuum. The thicknesses of the resulting dielectric films were 100−700 nm, as determined by ellipsometry.

(10) Bolze, J.; Kim, J.; Huang, J.-Y.; Rah, S.; Youn, H. S.; Lee, B.; Shin, T. J.; Ree, M. *Macromol. Res.* **2002**, *10*, 2.

(11) Londono, J. D.; Davidson, R. V.; Brill, D.; Roach, D. H.; Leach, R. A.; Quintana, J. P. *J. Appl. Crystallogr.* **2000**, *33*, 704.

(12) (a) Kinning, D. J.; Thomas, E. L. *Macromolecules* **1984**, *17*, 1712. (b) Pedersen, J. S. *J. Appl. Crystallogr.* **1994**, *27*, 595.

MA0501951